NO decomposition on an Mn-deposited Pd(100) surface

I. Nakamura, H. Hamada, and T. Fujitani *

Research Institute for Green Technology, National Institute of Advanced Industrial Science and Technology (AIST), Tsukuba, Ibaraki 305-8569, Japan

Received 1 November 2002; accepted 18 January 2003

The influence of Mn deposited on a Pd(100) surface on the adsorption, dissociation and desorption properties of NO has been studied using infrared reflection absorption spectroscopy (IRAS), temperature-programmed desorption (TPD) and X-ray photoelectron spectroscopy (XPS). On the Mn/Pd(100) surface, only the NO adsorbed on the Pd was observed at 320 K. Thermal dissociation of NO did not occur on the clean Pd(100) surface; it did occur, however, on the Mn/Pd(100) surface at 320 K. A Pd–Mn alloy was formed by deposition of Mn onto the Pd(100) surface; the formation of the Pd–Mn alloy was correlated with the activity of NO dissociation, assuming that it was the active site for this dissociation. The oxygen produced from the dissociation of NO was found to destroy the Pd–Mn alloy, forming MnOx. No desorption of oxygen from MnOx on Pd(100) was observed below 1200 K.

KEY WORDS: nitric oxides; decomposition; palladium; manganese; oxygen desorption; MnOx.

1. Introduction

The direct decomposition of NO to N_2 and O_2 over a solid catalyst is a very attractive reaction for removal of this pollutant from exhaust streams. Metal surfaces are known to be effective in catalyzing the elementary steps involved of adsorption and dissociation of NO, and desorption of N_2 and O_2 [1]. In particular, extensive studies have been conducted on the direct decomposition of NO over supported powder catalysts of noble metals such as Rh, Pt and Pd [2–4]. A serious problem for the direct decomposition of NO is the decreased activity due to oxidation of the catalyst surface by oxygen contained in the feed or produced by the dissociation of NO. Cu-ZSM-5 is the most effective catalyst for NO decomposition in the presence of oxygen [5]. A number of studies have focused on catalyst development for NO decomposition in the presence of oxygen [6]; however, no catalyst having a higher activity than Cu-ZSM-5 has yet been reported.

The influence of surface structure on NO decomposition on a noble metal single-crystal surface was examined using surface science techniques. On a Rh single-crystal surface [7–10], dissociation of NO on both flat and stepped surfaces has been reported, although the dissociation temperature (120–400 K) depends on the surface structure. Nitrogen and oxygen produced from the NO dissociation on the Rh surface desorb at 450–740 K and >830 K, respectively.

On a Pt single-crystal surface, the Pt(100) was active in the dissociation of NO, while Pt(111) and Pt(110) were inactive [11–14]. On the other hand, Masel's group reported that the stepped Pt surface was active in NO dissociation [12,15,16]. Banholzer and Masel found that the stepped Pt(410) surface showed NO dissociation percentage of >98% [15]. Furthermore, Pt(410) was found to be considerably more active for the NO dissociation than Pt(210), even though the step geometry is identical on the two surfaces and the step density is higher on Pt(210) [16]. It was concluded that the active site for NO decomposition on the Pt surface consists of a specific arrangement of atoms and is not just a step on the surface. It has been reported that both the NO dissociation and the desorption of nitrogen from the dissociated NO on the Pt surface occur at <500 K, while oxygen from the dissociated NO desorbs only at >700 K [11–13,15,16].

As for Pd single-crystal surfaces, the flat surface shows almost no activity for the dissociation of NO, while the stepped surface is active [17–19]. The NO dissociation and the desorption of nitrogen from dissociated NO on the stepped surface occur around 500 K, although no desorption of oxygen from the dissociated NO was observed below 1200 K [18]. It was thus clear that a higher temperature was needed for the desorption of oxygen produced from the dissociation of NO on a noble metal surface compared with the temperature of the NO dissociation or the desorption of nitrogen from the dissociated NO.

We have previously examined the effect of surface structure on the adsorption, dissociation and desorption properties of NO on Pd(100), (111) and (311) surfaces using infrared reflection absorption spectroscopy (IRAS) and temperature-programmed desorption (TPD) [20]. The dissociation of NO proceeds only on the stepped

* To whom correspondence should be addressed.
E-mail: t-fujitani@aist.go.jp

1011-372X/03/0400-0091/0

Pd(311) surface, where the desorption of N_2 is observed at 550 K, but no O_2 desorption was observed below 1200 K. Furthermore, the amount of NO adsorption on Pd(311) decreases with run number of the repeated adsorption and thermal dissociation of NO. The diffusion of oxygen from the dissociated NO into the subsurface or the bulk is observed on the stepped Pd(112) surface using high-resolution electron energy loss spectroscopy [18], assuming that the inhibition of NO adsorption by the repetition of the NO dissociation was due to the oxidation of the Pd by the oxygen incorporated into the subsurface or the bulk through the step sites of Pd(311).

It has been reported that Cu–Mn oxide powder catalysts are active in the direct decomposition of NO at room temperature [21]. Furthermore, the NO dissociation proceeds on an Mn-deposited Pd(100) surface below 300 K [22]. Theoretical calculations reveal that the N–O bond is weaker on the (111) and (100) surfaces of the Pd_3Mn alloy compared with the pure Pd metal surface, and hence that NO dissociates more easily on the alloy than on pure Pd [23]. Thus, the Mn-deposited Pd surface is effective for NO dissociation. However, the desorption behavior of the oxygen produced from the dissociation of NO has not been investigated. In this study, we have examined the effect of Mn deposited on the Pd(100) surface on the reactivity of NO together with the desorption characteristics of the oxygen produced from its dissociation using IRAS, TPD and X-ray photoelectron spectroscopy (XPS).

2. Experimental

The IRAS and TPD experiments were carried out in an ultrahigh-vacuum (UHV) apparatus composed of four chambers: a load-lock chamber for changing samples ($<2\times10^{-9}$ torr), a preparation chamber equipped with an ion gun for Ar^+ sputtering and an Mn deposition unit ($<4\times10^{-10}$ torr), a surface analysis chamber holding facilities for Auger electron spectroscopy (AES) and quadrupole mass spectroscopy ($<8\times10^{-11}$ torr), and a reaction chamber ($<9\times10^{-10}$ torr) in which the NO adsorption experiments were performed. An infrared spectrometer with a liquid nitrogen-cooled mercury–cadmium–telluride detector was situated next to the reaction chamber, allowing IRA spectra during the NO exposure to be obtained. The spectra were recorded at a resolution of $4\,cm^{-1}$ by 100 scans in a total measurement time of 30 s.

The XPS experiments were performed in a UHV apparatus composed of two chambers, a surface analysis chamber ($<2\times10^{-10}$ torr) and a preparation chamber ($<3\times10^{-8}$ torr). The analysis chamber was equipped with an ion gun for Ar^+ sputtering, a photoelectron analyzer for XPS and a doser for adjusting the NO exposure. An Mn deposition unit was situated in the preparation chamber. XPS spectra were measured with MgKα radiation.

The Pd(100) single-crystal disc (8 mm diameter, 1 mm thickness, 99.999% purity) was polished only on one plane. The accuracy of the crystal plane was within 1° and the surface roughness was $<0.03\,\mu m$. The Pd(100) surface was cleaned by Ar^+ sputtering at 1000 K for 10 min, annealed at 1000 K in 8×10^{-8} torr of oxygen for 15 min, then annealed at 1200 K in vacuum. The surface cleanliness of the sample was verified by AES and XPS. However, the AES peak of C(KLL) overlapped with the Pd(MNN) peak so the absence of carbon impurity was confirmed by noting the lack of CO and CO_2 thermal desorption following the adsorption of oxygen at room temperature.

The Mn was deposited onto the Pd(100) surface by electric heating of an Mn flake wrapped in tungsten foil. Varying the deposition time at a constant current controlled the amount of Mn. After the deposition of Mn, the sample was annealed at 873 K in vacuum for 5 min before the NO adsorption experiment. The adsorption of NO (99.9% pure) was carried out at 5×10^{-8} torr of NO exposure and a sample temperature of 320 K. The TPD experiments were performed at a 1.0 K/s heating rate.

3. Results and discussion

3.1. Adsorption and decomposition of NO on Mn-deposited Pd(100)

The effect of the Mn deposited on the Pd(100) surface on the adsorption and decomposition properties of NO was examined using IRAS and TPD. Figure 1 shows IRA spectra of NO adsorbed on Mn/Pd(100) surfaces with various Mn coverages (0–5.3 monolayer (ML)) during NO exposure at 320 K and 200 L. The peak of NO adsorbed on the two-fold bridge site was observed at $1666\,cm^{-1}$ for the clean Pd(100) surface [20]. Only the peak of NO adsorbed on Pd was observed for the Mn/Pd(100) surface. No new adsorption peak appeared after deposition of Mn. Further, we observed that the peak intensity of NO adsorbed on Mn/Pd(100) decreased with increasing Mn coverage, indicating that the number of Pd atoms exposed at the surface decreased with the deposition of Mn. No adsorption peak of NO was observed above 5 ML of Mn coverage, indicating that the surface Pd atoms were completely covered.

The TPD spectra of NO ($m/e=30$) and N_2 ($m/e=28$) after exposing the Mn/Pd(100) surface (0, 1.6, 3.5, 5.3 ML of Mn coverage) to 200 L of NO at 320 K are shown in figure 2. The NO desorption peak, but no N_2 desorption peak, was observed at 540 K for the clean Pd(100) surface, indicating that the thermal dissociation of NO does not occur [20]. In contrast, for Mn/Pd(100), N_2 was observed to desorb at ~750 K in addition to the desorption of NO, where no desorption peaks of O_2 or N_2O were observed below 1200 K. This clearly indicates

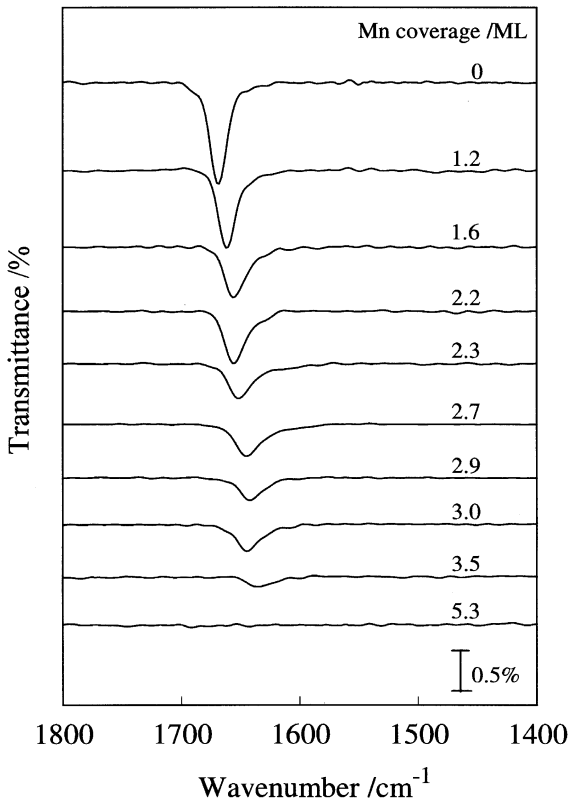

Figure 1. IRA spectra of NO adsorbed on Mn/Pd(100) surfaces with various Mn coverages (0–5.3 ML) during NO exposure at 320 K and 200 L.

that the dissociation of NO occurring on the Pd(100) surface is induced by the deposition of Mn. The NO adsorbed on the Pd of the Mn/Pd(100) surface was found to desorb near 480 K, i.e., about 60 K lower than the desorption temperature of NO adsorbed on the clean Pd(100) surface. This indicates that the binding energy of NO–Pd is weaker on Mn/Pd(100) than on

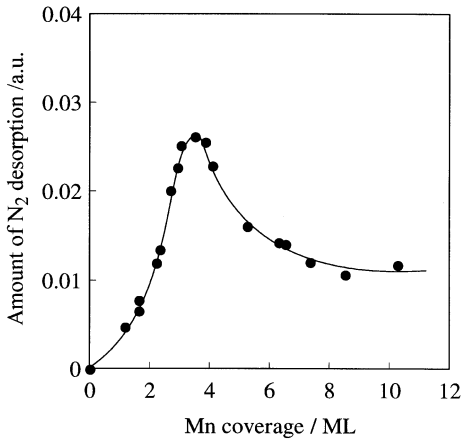

Figure 3. Amount of N_2 desorption from the Mn/Pd(100) surface as a function of Mn coverage after exposure to 200 L of NO at 320 K.

Pd(100). This result is in accordance with theoretical calculations predicting that NO adsorbed on a $Pd_3Mn(100)$ surface is less strongly bound than on pure Pd, because a small magnetic moment remains on NO adsorbed on the surface [24].

Figure 3 shows the amount of N_2 desorption from the Mn/Pd(100) surface as a function of Mn coverage after exposure to 200 L of NO at 320 K. The amount of N_2 desorption increased with Mn coverage below 3.5 ML and decreased between 3.5 and 7 ML. The optimum Mn coverage for the dissociation of NO was 3.5 ML, indicating that both Pd and Mn atoms produced effective sites for the NO dissociation. The amount of N_2 desorbed at 3.5 ML of Mn coverage corresponded to about 0.5 ML of nitrogen coverage, in agreement with that formed by the thermal dissociation of saturated NO on Pd(311) at 320 K. Above 7 ML of Mn coverage, where the surface was completely covered by Mn, the activity for the NO

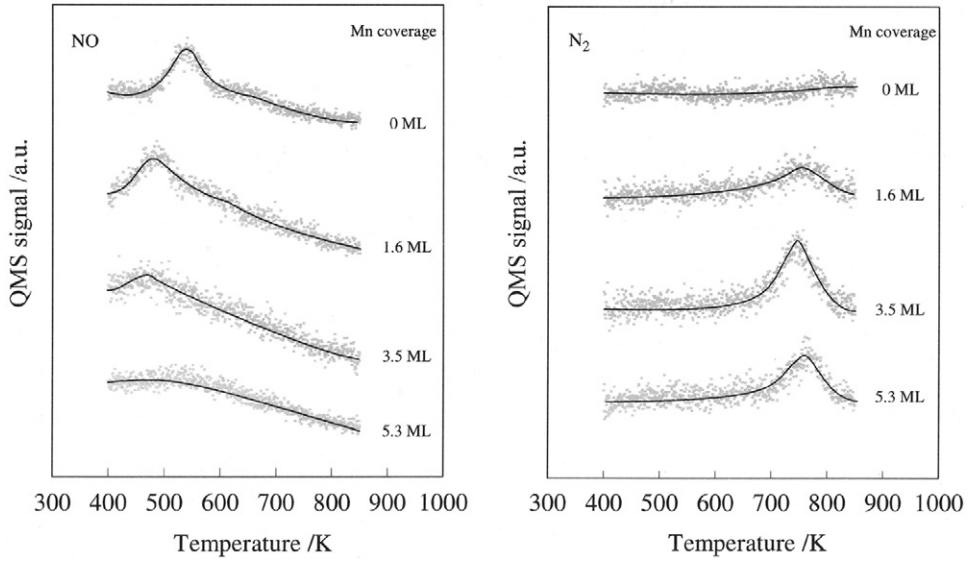

Figure 2. TPD spectra of NO ($m/e = 30$, left) and N_2 ($m/e = 28$, right) after exposing the Mn/Pd(100) surface (0, 1.6, 3.5, 5.3 ML of Mn coverage) to 200 L of NO at 320 K.

dissociation became almost constant, indicating that the dissociation of NO occurred on the surface of the Mn alone.

The amount of NO adsorption decreased with increased Mn coverage as shown in figure 1, while the amount of N_2 desorbed increased with the Mn coverage below 3.5 ML. This result indicates that the dissociation of NO occurs during the NO exposure at 320 K. Sandell *et al.* [25] have also reported that NO adsorbed molecularly on 0.7 ML Mn/Pd(100) at 100 K dissociates upon heating to 325 K. Using photoelectron spectroscopy, they confirmed N_a and O_a on the surface resulting from NO dissociation.

It was found that the dissociation of NO proceeded on the Mn/Pd(100) surface below 320 K, while the N_2 desorption by the recombination of dissociated nitrogen occurred at 750 K regardless of Mn coverage as shown in figure 2. On the other hand, we have previously examined the adsorption, dissociation and desorption properties of NO on the stepped Pd(311) surface [20]. The nitrogen produced from NO dissociation on the stepped Pd surface was shown to desorb at 550 K, where the NO molecularly adsorbed at 320 K. It was thus found that the Mn/Pd(100) surface had a high dissociation activity of NO at low temperature compared with the stepped Pd surface, while the N_2 desorption from the Mn/Pd(100) surface required a 200 K higher temperature compared with that from the stepped Pd surface.

3.2. Surface analysis by XPS

The surface analysis for Mn/Pd(100) before and after the NO exposure was carried out by XPS. Figure 4 shows the Pd $3d_{5/2}$ and Mn $2p_{3/2}$ spectra of Mn/Pd(100) with various Mn coverages taken before the NO exposure. In the Pd $3d_{5/2}$ spectra, one peak was observed at 335.3 eV and another at 336.3 eV. The peak at 335.3 eV, which agreed with the binding energy of the Pd $3d_{5/2}$ peak for the clean Pd(100) surface, was identified as metallic Pd. Previous work has shown that the Pd $3d_{5/2}$ peak for the Pd–Mn alloy shifts about 1 eV toward higher binding energy compared with that for metallic Pd [22,25]. The peak at 336.3 eV could be identified as Pd in the Pd–Mn alloy. The deposition of Mn on the Pd(100) surface results in the formation of a Pd–Mn alloy.

In the Mn $2p_{3/2}$ spectra, one peak appeared at 639.0 eV and another at 640.2 eV. The peak at 639.0 eV was assigned to metallic Mn based on literature data [26]. As no oxygen species were detected on the surface before NO exposure, it was evident the other 640.2 eV peak could not be due to the Mn oxide, although the binding energy was close to that of MnO (640.5–641.4 eV) [26]. The peak is tentatively assigned to Mn in the Pd–Mn alloy.

Figure 5 shows the N 1*s* and O 1*s* spectra for Mn/Pd(100) after the NO exposure at 320 K. Peaks due to atomic nitrogen and oxygen formed by the NO dissociation were observed at 396.5 and 530.0 eV, respectively [25]. This indicates that the NO dissociates on the Mn/Pd(100) surface at 320 K. In addition, the amount of atomic nitrogen was well correlated with that of the N_2 desorption from the Mn/Pd(100) surface (figure 3).

The Pd $3d_{5/2}$ and Mn $2p_{3/2}$ spectra of Mn/Pd(100) with various Mn coverages taken after the NO exposure at 320 K are shown in figure 6. In the Pd $3d_{5/2}$ spectra, two peaks due to the metallic Pd and Pd in the Pd–Mn alloy were observed at 335.3 and 336.3 eV, respectively. These binding energies agreed with those before the NO exposure (figure 4); however, the peak area ratio of Pd for the Pd–Mn alloy/metallic Pd was smaller than that before NO exposure for every Mn coverage investigated. In the Mn $2p_{3/2}$ spectra, on the other hand, one peak was observed at 639.0 eV and another at 640.4 eV.

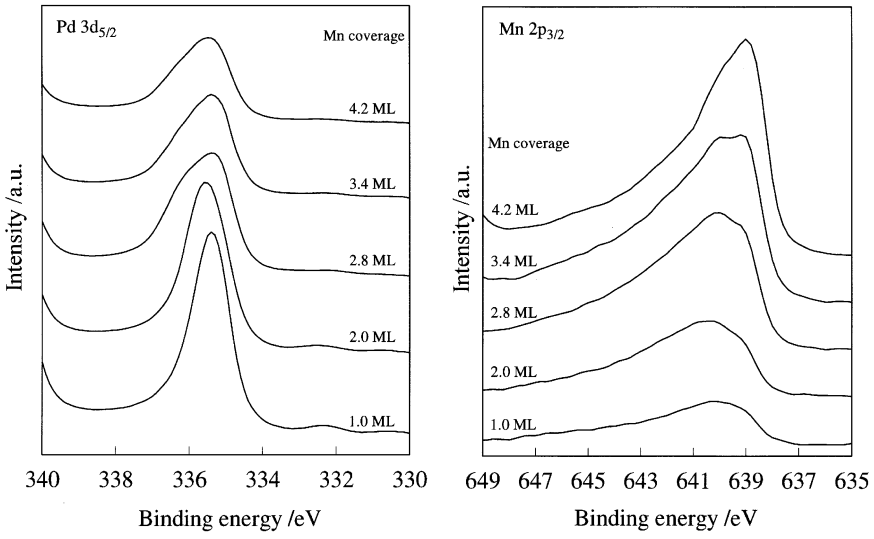

Figure 4. Pd $3d_{5/2}$ and Mn $2p_{3/2}$ spectra of Mn/Pd(100) with various Mn coverages taken before the NO exposure.

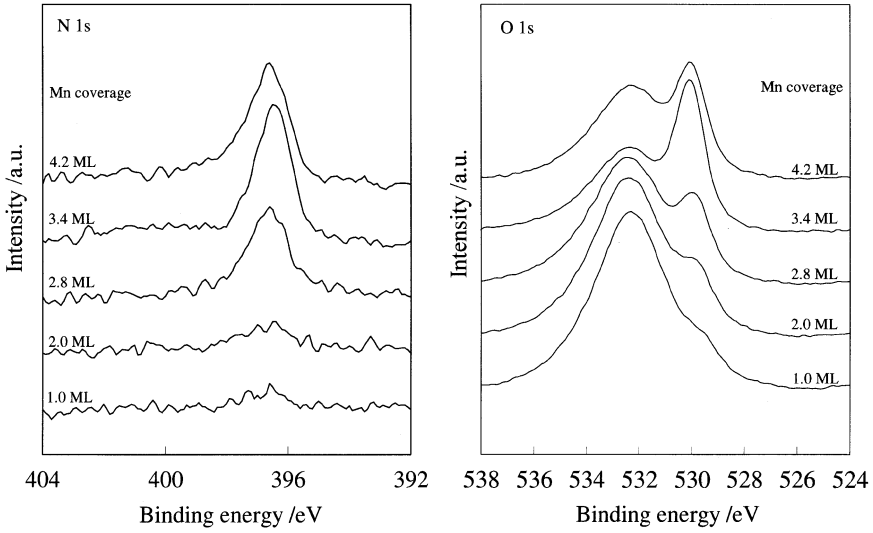

Figure 5. N 1*s* and O 1*s* spectra for Mn/Pd(100) after the NO exposure at 320 K.

In this case, the metallic Mn ratio (630.9 eV) became small compared with that before NO exposure. The proportion of Pd–Mn alloy and metallic Mn on the Mn/Pd(100) surface decreased on exposure to NO at 320 K.

The oxygen produced by dissociation of NO was detected on the Mn/Pd(100) surface as shown in the O 1*s* spectra (see figure 5). The dissociated oxygen on the clean Pd(100) surface after dosing with O_2 began to desorb from 800 K. However, no desorption of the oxygen from dissociated NO on Mn/Pd(100) was observed below 1200 K, and the O 1*s* peak was detected even after TPD. We conclude that this oxygen is bound to Mn. Furthermore, the 640.4 eV peak became broad compared with that before the NO exposure, indicating that the Mn was oxidized to MnOx. It appears that the Pd–Mn alloy was converted to MnOx by oxygen arising from the dissociation of NO.

3.3. Pd–Mn alloy

The coverages of the Pd (336.3 eV) and the Mn (640.2 eV) for the Pd–Mn alloy forming on the Pd(100) surface before the NO exposure (figure 4) as a function of Mn coverage are plotted in figure 7. The coverage of the Pd for the Pd–Mn alloy increased with Mn coverage up to about 3 ML and decreased above 3 ML. This feature was similar to that of the N_2 desorption from the Mn/Pd(100) surface as shown in figure 3, assuming that the Pd–Mn alloy was the active site for the dissociation of NO. The decrease of the Pd–Mn alloy above 3 ML is probably due to the covering by metallic Mn. Furthermore, the coverages of the Pd and the Mn for the Pd–Mn alloy were found to exhibit a similar dependence on Mn coverage. This strongly supported the assignment of the Mn $2p_{3/2}$ peak at 640.2 eV to Mn in the Pd–Mn alloy. The ratios of Pd and Mn for the

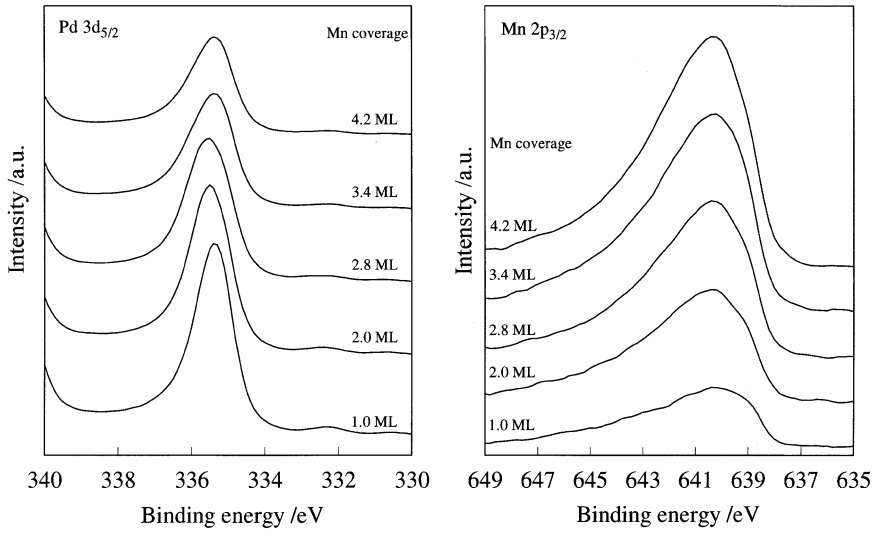

Figure 6. Pd $3d_{5/2}$ and Mn $2p_{3/2}$ spectra of Mn/Pd(100) with various Mn coverages taken after the NO exposure at 320 K.

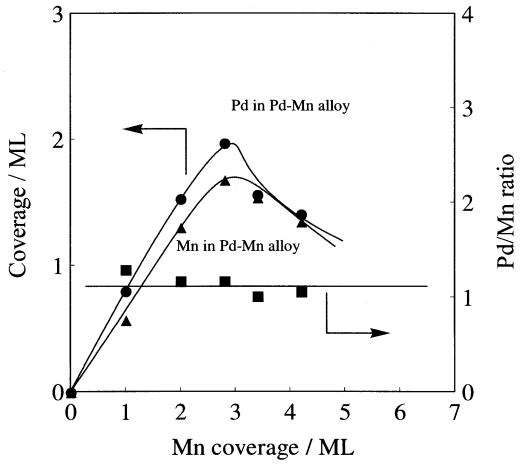

Figure 7. Coverages of Pd (336.3 eV) and Mn (640.2 eV) for the Pd–Mn alloy forming on the Pd(100) surface before the NO exposure as a function of Mn coverage.

Pd–Mn alloy were almost equal (figure 7), which was consistent with that for a c(2 × 2) Pd–Mn alloy observed on Mn-deposited Pd(100) by LEED [22,25,27,28] and STM [25,28].

As shown in figure 6, the Pd–Mn alloy was destroyed by the oxygen produced from the dissociation of NO, forming MnOx. In order to clarify the influence of the MnOx on NO decomposition, the amount of N_2 desorption from Mn/Pd(100) at 2.3 ML of Mn coverage was examined for each run number of repeated NO exposure and thermal desorption. In run 2, the amount of N_2 desorption declined to half of its initial value; it reached zero in run 3. The activity of NO decomposition was shown to decrease with run number. It was thus found that the activity of NO decomposition decreased with the formation of MnOx. This result strongly suggests that the Pd–Mn alloy is the active site for NO dissociation.

4. Conclusions

(1) Thermal dissociation of NO does not proceed on a clean Pd(100) surface. Dissociation of NO occurs at 320 K after deposition of Mn onto the Pd(100) surface.

(2) Surface analysis using XPS shows that a Pd–Mn alloy is formed by deposition of Mn onto the Pd(100) surface. The coverage of the Pd–Mn alloy was correlated with the activity of NO dissociation, assuming that the Pd–Mn alloy was the active site.

(3) The Pd–Mn alloy was destroyed by oxygen produced from the dissociation of NO, forming MnOx; the activity of NO decomposition decreased with the formation of MnOx. No desorption of oxygen from the decomposition of MnOx on Pd(100) was observed below 1200 K.

References

[1] W.A. Brown and D.A. King, J. Phys. Chem. B 104 (2000) 2578.
[2] K. Almusaiteer, R. Krishnamurthy and S.S.C. Chuang, Catal. Lett. 55 (2000) 291.
[3] A. Gervasini, P. Carniti and V. Ragaini, Appl. Catal. B 22 (1999) 201.
[4] S. Lacombe, J.H.B.J. Hoebink and G.B. Marin, Appl. Catal. B 12 (1997) 207.
[5] M. Iwamoto, N. Mizuno and H. Yahiro, Sekiyu Gakkaishi 34 (1991) 375.
[6] M. Iwamoto and H. Hamada, Catal. Today 10 (1991) 57.
[7] L.H. Dubois, P.K. Hansma and G.A. Somorjai, J. Catal. 65 (1980) 318.
[8] L.A. Delouise and N. Winograd, Surf. Sci. 159 (1985) 199.
[9] H.A.C.M. Hendrickx and B.E. Nieuwenhuys, Surf. Sci. 175 (1986) 185.
[10] A. Siokou, R.M. van Hardeveld and J.W. Niemantsverdriet, Surf. Sci. 402–404 (1998) 110.
[11] R.J. Gorte, L.D. Schmidt and J.L. Gland, Surf. Sci. 109 (1981) 367.
[12] J.M. Gohndrone and R.I. Masel, Surf. Sci. 209 (1989) 44.
[13] D.Y. Zemlyanov, M.Y. Smirnov, V.V. Gorodetskii and J.H. Block, Surf. Sci. 329 (1995) 61.
[14] T.H. Lin and G.A. Somorjai, Surf. Sci. 107 (1981) 573.
[15] W.F. Banholzer and R.I. Masel, J. Catal. 85 (1984) 127.
[16] J.M. Gohndrone, Y.O. Park and R.I. Masel, J. Catal 95 (1985) 244.
[17] S.W. Jorgensen, N.D.S. Canning and R.J. Madix, Surf. Sci. 179 (1987) 322.
[18] R.D. Ramsier, Q. Gao, H. Neergaard Waltenburg, K.-W. Lee, O.W. Nooij, L. Lefferts and J.T. Yates, Jr., Surf. Sci. 320 (1994) 209.
[19] M. Hirsimäki, S. Suhonen, J. Pere, M. Valden and M. Pessa, Surf. Sci. 402–404 (1998) 187.
[20] I. Nakamura, T. Fujitani and H. Hamada, Surf. Sci. 514 (2002) 409.
[21] I. Spassova, M. Khristova, N. Nyagolova and D. Mehandjiev, Stud. Surf. Sci. Catal. 130 (2000) 1313.
[22] A. Sandell, A.J. Jaworowski, A. Beutler and M. Wiklund, Surf. Sci. 421 (1999) 116.
[23] F. Delbecq, B. Moraweck and L. Vérité, Surf. Sci. 396 (1998) 156.
[24] F. Delbecq and P. Sautet, Surf. Sci. 442 (1999) 338.
[25] A.J. Jaworowski, R. Ásmundsson, P. Uvdal, S.M. Gray and A. Sandell, Surf. Sci. 501 (2002) 83.
[26] B. Bozzini, E. Griskonis, A. Fanigliulo and A. Sulcius, Surf. Coat. Technol. 154 (2002) 294.
[27] D. Tian, R.F. Lin, F. Jona and P.M. Marcus, Solid State Commun. 74 (1990) 1017.
[28] A.J. Jaworowski, S.M. Gray, M. Evans, R. Asmundsson, P. Uvdal and A. Sandell, Phys. Rev. B 63 (2001) 125401.